# ADDITIVE MANUFACTURING BY ROBOT MANIPULATOR: AN OVERVIEW OF THE STATE-OF-THE-ART AND PROOF-OF-CONCEPT RESULTS

Linn Danielsen Evjemo[1], Signe Moe[1], Jan Tommy Gravdahl[1], Olivier Roulet-Dubonnet[2], Lars Tore Gellein[2], and Vegard Brøtan[3].

***Abstract*— For the last decades, additive manufacturing (AM) has become an ever increasing part of the development of new technology and devices. However, it is still challenging to use this technology on a larger scale. This paper presents the state-of-the-art of large-scale AM, looking into some of the projects that have come furthest in utilising AM technology on large structures such as buildings or sculptures. The background for this research is to consider the possibility of large-scale AM by robot manipulator using the welding method cold metal transfer (CMT). After outlining the the necessary algorithms and components for such an AM system, a proof-of-concept experiment using a UR5 robot is presented. This initial experiment will clarify some of the challenges that need to be addressed in future work.**

## I. INTRODUCTION

Additive manufacturing (AM) is an umbrella term for several specific techniques that primarily build up structures layer by layer, and which often go by names such as free-form fabrication, rapid prototyping (RP), or 3D-printing [1]. AM is the most general term, and will be used throughout this article. AM technology has made it easier for small companies and individual developers to make custom made parts at a reasonable price, and it has also made prototyping easier and less expensive. While AM has mostly been used for creating smaller parts for larger products or processes, the process has also been used to create small end products.

Typically, AM is time demanding for larger components. This is because the production layer size affects the roughness and accuracy of the constructed surfaces. With low layer thicknesses, the AM-machines are often restricted to small build volumes, as larger volumes tend to take an unreasonable amount of time. However, in many cases machining or other surface treatments are necessary to get the desired surface properties for the end product. In such parts where surface quality and detail are less important, it is possible to build quicker and bigger. For traditional AM-processes, this implies that the machines need to grow to a larger scale than the produced parts, which in any case would limit the build volume.

One way of enabling additive manufacturing of large-scale products ”outside the box”, is to combine AM with robotics. By using a robot manipulator to extrude a fast-curing material, gradually building up a larger structure, the workspace for the build would be massively expanded. Most of the flexibility for the shape and form of the final product that traditional AM-methods allows for should be kept or even improved, as parameters like build speed, layer thickness, and even nozzle size would allow for changing build speed between the general production and finer details. If the build material is metal, or some other very fast-curing material, the need for support structures could also decrease to the point of only relying on anchoring and stabilising. If necessary, it would also be possible to increase the flexibility of the building process itself, because the structure would no longer have to be built layer by layer from the bottom-up or top-down - which is necessary for most existing forms of AM. Several robot manipulators could potentially also work simultaneously, building with several different materials.

In this paper, we will present an overview of current approaches to AM by robot, as well as a novel concept of using an industrial robotic manipulator as a means for 3D-printing or AM. We will outline the necessary algorithms and components needed to realise such a system. The paper is organized as follows: In section II, an overview of the current approaches to large-scale AM by robot will be presented. In section III, we will explain our novel idea of AM by robot manipulator. A proof-of-concept experiment is presented in section IV, and the results as well as plans for future work are summarized in section V.

## II. AN OVERVIEW OF CURRENT TECHNOLOGY

Several projects are already working on realising robotised AM, both with generic materials like plastic or cement, and with metal. Most of these projects are initiated by private businesses, but there are also a few universities working on this kind of technology.

One way of creating large structures through AM methods is by splitting the final product into smaller parts that can be 3D-printed, and then assemble the pieces afterwards. This has been done for example for the 3D Elephant Petition [2], Total Kustom’s concrete castle [3], and to some extent the Dragon Bench from Joris Laarman Lab [4].

[1]Linn Danielsen Evjemo, Signe Moe, and Jan Tommy Gravdahl are with the Department of Engineering Cybernetics, NTNU, Trondheim, Norway {linn.d.evjemo, signe.moe, jan.tommy.gravdahl}@ntnu.no

[2]Olivier Roulet-Dubonnet and Lars Tore Gellein are with SINTEF Raufoss Manufacturing AS, Trondheim, Norway {Olivier.Roulet-Dubonnet, Lars.Tore.Gellein}@sintef.no

[1]Vegard Brøtan is with the Department of Mechanical and Industrial Engineering, NTNU, Trondheim, Norway {vegard.brotan}@ntnu.no


Fig. 1. **3D Elephant Petition:** The pieces that make up the 3D-printed elephant sculpture were made by five traditional Ultimaker 3D-printers. Each of these printers were given an extended degree of freedom by connecting them to a rail that moved vertically, which made it possible to print pieces that were up to 2.5 meters tall. Photo: www.rooiejoris.nl [2].

The 3D Elephant Petition, created by Joris van Tubergen in 2014, took traditional 3D-printing one step further in the process of 3D-printing large structures ”outside-the-box”. As part of an art project, he created a life-scale 3D-printed elephant sculpture over the course of two weeks. He did this by combining five Ultimaker 3D printers with his own add-on called Z-Unlimited [5]. This add-on allowed each printer to move over 2.5 meters vertically while printing horizontally. This extended degree of freedom enabled the system to print structures that were over 2.5 meters tall. The remaining dimensions for each piece were still limited to the dimensions of the Ultimaker 3D-printer's original workspace. Even though the 3D-printed pieces were larger than what what a standard Ultimaker 3D-printer can produce, the final structure shown in figure 1 had to be assembled manually.

In 2006, two researchers from Cornell University developed and released an open-source, low-cost print-at-home system called Fab@Home [6]. This was done in an effort to make AM technology more available for developers, and encourage the invention of new technology. This was a three-axis gantry positioning system that used a syringe-based extrusion tool to do material extrusion along a translation-only path. The printer was designed so that it was possible to use a great variety of materials, for instance RTV silicone rubber, epoxy, and even chocolate. Model 2 was released in 2009, with improvements like a more versatile material extrusion system, as well as a price reduction due to changes in the electronics and mechanics [7].

The company Total Kustom are working on large-scale 3D-printing of houses, as part of an effort to help the construction of more affordable housing. They have 3D-printed large structures of cement with their own 3D Concrete Printing Technology, like the concrete castle that was built in 2014 [3], shown in figure 2. Their first construction was printed piece by piece, and then assembled manually. The castle was build using a cement mix, and the layers were 10 mm in height and 30 mm in width [8]. The project later 3D-printed an entire hotel suite, this time in one piece [9]. According to their website, they are now going into production of the first commercially available 3D Concrete Printers [10]. The largest models will have a workspace of approximately 150 m$^2$, and build structures that are up to 12 m tall, with an average printing speed of 100 m$^2$ in area and 3 m height in 48 hours [11].

Fig. 2. **Concrete Castle:** This castle was built in cement in 2014 using Total Kustom's AM technology. This was their first large project, and the structure was therefore built piece by piece, and then assembled afterward. Photo: www.totalkustom.com [12].

Fig. 3. **Apis Cor House:** The robot manipulator used in their project is similar to a tower crane, with a workspace in a circular area around its base. Photo: www.totalkustom.com [14].

Apis Cor company recently managed to 3D-print a complete house in Moscow Region, using a self-developed mobile system for AM. They used a concrete mixture as building material, and built using a robot manipulator similar to a tower crane, as shown in figure 3. Their printer weighs around 2 tonns, has a maximum working area of 132m$^2$ in a circular area around the base, and can build structures that are up to 3300 mm tall [13]. The printer uses the traditional bottom-up approach, and deposits material layer by layer. The printed house was 38 m$^2$, and built in 24 hours of machine printing time [14].

Large-scale AM with a cable-suspended robot has also been tested, with promising results. In 2015, researchers from the University of Laval in Canada used AM to build a life-size foam statue of Sir Wilfrid Laurier, the seventh Prime Minister of Canada [15]. They used a 6 degrees of freedom (DOF) cable-suspended robot in the process, a type of robot that is attached to a mobile platform or end effector by multiple cables. The final statue was about $215 \times 550 \times 620$ mm large, printed with material laid out in a path that was 10 mm tall and 12 mm wide. The whole print was done with the end-effector pointing in the same direction, making this a translation-only build. For traditional 3D-printers, this type of print would be possible with only 3 DOFs, because the end-effector's orientation never changes. However, for a cable-suspended robot, 6 DOFs are necessary to keep the orientation of the end effector unchanged. This project was inspired by the work done by researchers from Ohio University in 2007, who created a cable-suspended contour crafting system. Their motivation was that building large structures with a gantry robot, a large overhanging system covering the whole work area, is difficult because the robot must be extremely large, heavy, and difficult to move around. A cable-suspended system also has to be larger than the structure it is building [16], but it is more mobile because the cable frame is much lighter than a complete gantry robot system. Still, a gantry robot-system is much more accurate than a cable-system.

The Norwegian company Norsk Titanium (NTi) has developed a method for cost-efficient AM of titanium airplane parts. Traditionally, titanium parts are created by subtracting material from a large, wrought titanium block until the desired shape is achieved using a 3 axis manipulator in a confined box with inert gas. Components that require a lot of machining becomes more costly and produces much more waste compared to NTis method. By fusing titanium wire together in an atmosphere of argon gas, NTi are able to build up titanium parts layer by layer [17]. Even though this process demands that the AM parts are machined afterwards, this process saves both time and material. NTi's system currently has a workspace of $120 \times 120 \times 180$ cm [18], which is quite large compared to traditional 3D-printers.

One of the projects that has come furthest in combining AM and robotics, is the work done by Joris Laarman Lab. They have moved, step by step, from using AM as a design tool and over to building structures directly with AM methods. Early projects like the Bone Chair from 2006 [19] used AM to create complex molds for design furniture that were to be casted in one piece [20].

The MX3D Metal printer must be the most exciting thing to come out of Joris Laarman Lab yet. This was a further development of the Mataerial project from 2012 [21], where a 6 DOF industrial robot manipulator was used to deposit material along a pre-designed trajectory. The Mataerial project was a collaboration between Joris Laarman Lab and the Institute of Advanced Architecture of Catalonia (IAAC), and resulted in a patented AM method for building fast-curing thermoplastic in any direction: no longer limited to the top-down or bottom-up approach. This made it possible to build almost any kind of structure, with no need for support or underlying layers, like shown in figure 4.

By combining the industrial robot manipulator as used in the first Mataerial project with an advanced welding machine, Joris Laarman Lab were able to build structures in metals such as steel, aluminium, bronze, stainless steel, and copper.

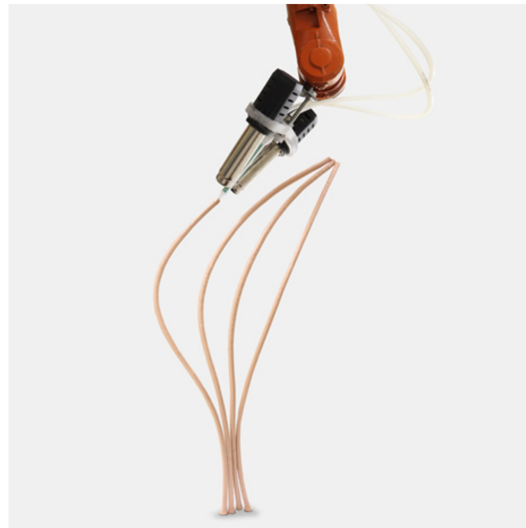

Fig. 4. **Mataerial project:** Combining an industrial manipulator with a fast-curing plastic makes it possible to ”print” double curved lines in mid-air. Photo: www.mataerial.com [21].

Fig. 5. **Butterfly Screen:** This $2 \times 3$ meter large double-curved bronze screen is built by an industrial robot manipulator using the MX3D AM technology. Photo: www.jorislaarman.com [23].

This robot is able to build double-curved lines in midair by depositing small amounts of molten metal at a time. The Dragon bench from 2014 was built piece by piece, and later welded together manually [4]. The Butterfly Screen on the other hand, shown in figure 5, is a $2 \times 3$ meter large double curved bronze structure that was built as a whole using the MX3D AM technology. Joris Laarman Lab are aiming to create an AM system that can eventually print structures directly from Computer Aided Design (CAD). MX3D have announced that they plan to use their AM method to build a one-piece, fully functional steel bridge sometime in 2017. The structure will be built at a work-site near their offices in Amsterdam, and will be placed across the Oudezijds Achterburgwal Canal [22].

## III. AM USING CMT BY 6 DOF ROBOT MANIPULATOR

Our research plan on using a robot manipulator to do AM in metal. More specifically, the aim is to use the welding method Cold Metal Transfer (CMT) to deposit metal along a given trajectory, building the final metal structure gradually as the manipulator tracks this reference trajectory. CMT is a metal inert gas (MIG) process which is modified so that the motions of the wire is integrated in the welding process. The need of an extra electromagnetic force is removed by using a wire retraction motion to help the metal droplet detachment. This means that both heat input and spatter can be decreased compared to other MIG methods [24]. CMT was chosen over other welding methods due to its high quality string, which is expected to be a decisive factor in additive manufacturing based on welding.

Mounting it on an industrial 6 DOF robot was a logical choice to enable building large objects. Combining CMT welding with robotised AM has the potential to build metal structures from scratch, not just perform robotised welding. However, this technology could also be useful in repair work, for example when needing to close holes and tears in large metal surfaces on ships or other large structures. The usual argument against industrial robots for AM is their limited precision, but metal welding is a comparatively rough process, so robot precision is not expected to be the limiting factor for product quality. AM by robot manipulator would free us from having to build structures layer by layer, which makes it possible to print more complex geometries. Being able to print in any direction may also make it possible to design more efficient path planning algorithms, which can potentially save both time and money.

In order to create a system for CMT-focused robotised AM, there are several problems that need to be solved. Path planning algorithms must be designed, planning the path the robot should follow while depositing material. These should be designed so that they can be used for a number of different building materials, as it will be useful to run tests with materials that are easier to deposit than metal. Control algorithms for the robot manipulator should be improved to account for feedback from the build process and the deposited material. The control algorithms will have to rely upon the properties of the given material, the thickness of the material line that is deposited, and on how fast the material hardens. It is therefore necessary to consider the time aspect, i.e. how fast it is possible to deposit the material, and how long it will take to build the complete structure.

Methods for collision avoidance must also be included in the system, something that might prove especially challenging if the system is to deviate from the standard bottom-up or top-down building approach. Throughout the process, it will be necessary to create experiment(s) with robot manipulator and deposition of material in order to test the control algorithms that are designed.

## IV. PROOF OF CONCEPT EXPERIMENT

Building on our previous experience with robotic set ups [25], a small-scale proof-of-concept experiment was designed. After considering alternatives like a glue gun, or even the print head of a traditional 3D-printer, a caulking gun of the type *Juniorfix* from Würth was chosen to deposit material.


Fig. 6. **Experiment set-up:** A caulking gun driven by compressed air is connected in parallel to the end effector of a UR-5 robot arm.

This alternative was deemed the best choice for a small-scale, initial experiment like this. In addition, the different materials that were available for the caulking gun had properties that made them better suited than for instance hot glue. These materials were typically less liquid than hot glue, and would behave in a more manageable way. The layers of hot glue would for instance just blend into each other if the layers were deposited too close together, and too quickly. The idea of using the print head of a 3D-printer was discarded partly because it would complicate the experimental set-up, and partly because it was necessary to have the opportunity to extrude more material at once than what one can expect with a traditional 3D-printer. A 3D-printer would almost certainly have been able to build a more accurate structure, but the main requirement of this experiment was build-time and simplicity, not accuracy.

The caulking gun was driven by compressed air, which created a smooth and constant flow of material once the pressure was turned on. The flow of compressed air was controlled by a valve that had to be operated manually. The material used was STP Quickfast from Würth, which is a type of fast-hardening, viscous glue. The caulking gun was fastened to the end of a UR-5 robot as shown in figure 6, with the nozzle parallel to the end effector of the robot arm. The trigger button of the caulking gun was strapped in place so that the extrusion of material was controlled directly by supplying compressed air. Because the nozzle was circular, the extruded material also had a circular cross-section, and the diameter was set by changing the diameter of the nozzle.

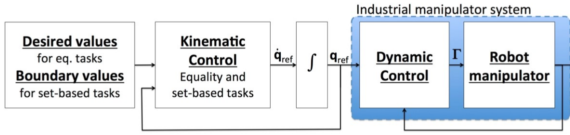


Fig. 7. **Control structure of the system:** The control algorithm is implemented in the block for kinematic control. Figure from [25].

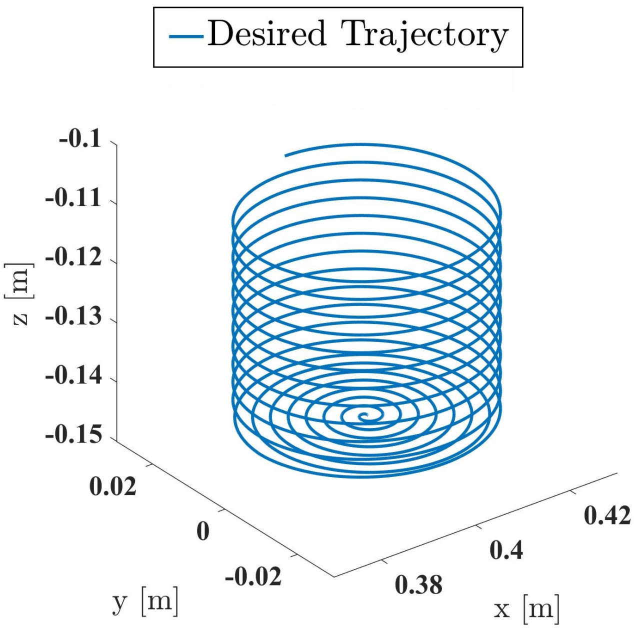


Fig. 8. **UR5 Trajectory:** Here we see a plot of the trajectory the robot's end effector should follow while depositing material along its path.

## A. TRAJECTORY DESIGN

The goal of the experiment was to construct a small cup, and the trajectory was designed such that the robot motion was continuous also as the nozzle moved upwards while printing the sides of the cup. This already deviates from traditional AM methods, which as a norm build one layer at a time and then move up (or down) a certain height before printing the next layer. This added flexibility can potentially allow for a more efficient building process in terms of both time and energy.

Each point on the spiral trajectory is expressed in cylindrical coordinates $\theta$, $r$, and $z$. We define $h$ as the height difference between each layer of the cup size, and $r_1$ as the horizontal distance between each layer of the bottom. $H$ is the desired final height of the structure, and $R$ is the desired radius of the final structure. All of these variables are given in meters. $r$ and $z$ are defined as functions of $\theta$:

$$r(\theta) = \begin{cases} \frac{r_1}{2\pi}\theta & \theta \leq \frac{R}{r_1}2\pi \\ R & \theta > \frac{R}{r_1}2\pi \end{cases} \tag{1}$$

$$z(\theta) = \begin{cases} 0 & \theta \leq \frac{R}{r_1}2\pi \\ \frac{h}{2\pi}(\theta - \frac{R}{r_1}2\pi) & \theta > \frac{R}{r_1}2\pi \end{cases} \tag{2}$$

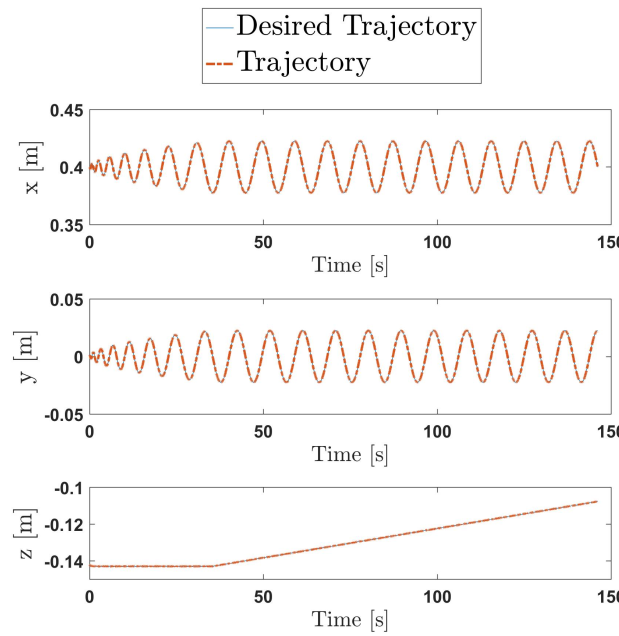


Fig. 9. **Translation error:** Here we see the desired x-, y-, and z-position plotted together with the actual position of the robot manipulator's end effector during one of the builds. The Cartesian coordinates are given in the robot frame.

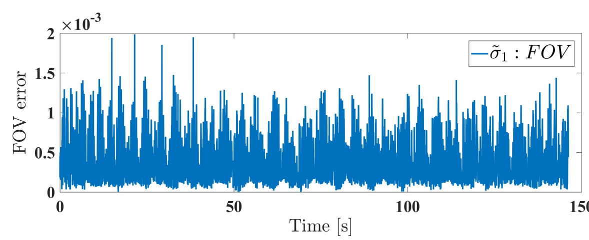


Fig. 10. **Field-of-view error:** The registered error between the actual field-of-view and the desired field-of-view is less than 2 $\times 10^{-3}$.

Thus, the time-derivatives of $r_1$ and $z$ are given by:

$$\dot{r}(\theta) = \begin{cases} \frac{r_1}{2\pi}\dot{\theta} & \theta \leq \frac{R}{r_1}2\pi \\ 0 & \theta > \frac{R}{r_1}2\pi \end{cases} \tag{3}$$

$$\dot{z}(\theta) = \begin{cases} 0 & \theta \leq \frac{R}{r_1}2\pi \\ \frac{h}{2\pi}\dot{\theta} & \theta > \frac{R}{r_1}2\pi \end{cases} \tag{4}$$

where $\dot{\theta}$ is defined as:

$$\dot{\theta} = \begin{cases} \frac{2\pi U}{r_1\sqrt{\theta^2+1}} & \theta \leq \frac{R}{r_1}2\pi \\ \frac{U}{\sqrt{R^2+\frac{h}{2\pi}^2}} & \theta > \frac{R}{r_1}2\pi \end{cases} \tag{5}$$

$\dot{\theta}$ is chosen such that the end effector velocity along the trajectory is constant and equal to the desired velocity $U$, which is necessary for even deposition of the printing

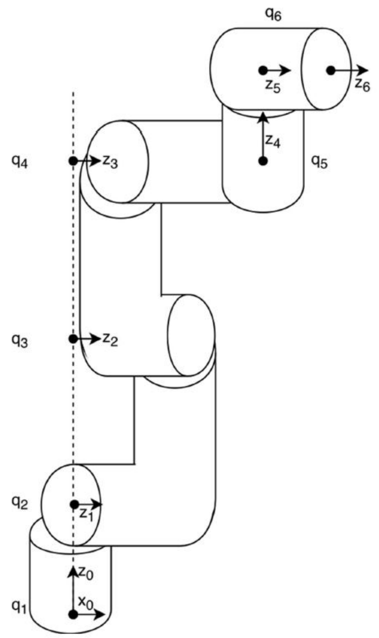


Fig. 11. **UR 5 Manipulator:** Here we see the coordinate frames assigned to the robot's joints, which is the foundation for the Denavit-Hartenberg parameters presented in table I. Figure from [25].

TABLE I
DENAVIT-HARTENBERG PARAMETERS FOR UR5, FOUND IN [26].

| Joint | $a_i$ [m] | $\alpha_i$ [rad] | $d_i$ [m] | $\theta_i$ [rad] |
|---|---|---|---|---|
| 1 | 0 | $\frac{\pi}{2}$ | 0.089 | $q_1$ |
| 2 | -0.425 | 0 | 0 | $q_2$ |
| 3 | -0.392 | 0 | 0 | $q_3$ |
| 4 | 0 | $\frac{\pi}{2}$ | 0.109 | $q_4$ |
| 5 | 0 | $-\frac{\pi}{2}$ | 0.095 | $q_5$ |
| 6 | 0 | 0 | 0.082 | $q_6$ |

material.

Figure 8 shows the designed trajectory the robot's end effector should follow. In figure 9 we see the desired x-, y-, and z-coordinates plotted together with the actual coordinates from the robot, and in figure 10 we see the error of the field-of-view $\sigma_{fov}$, defined in (14).

### B. ROBOT CONTROL

In this experiment, a UR-5 robot with 6 DOFs was used. Its configuration is given by $q = [q_1, q_2, q_3, q_4, q_5, q_6]^T$, $q_i$ being the joint variables. The Denavit-Hartenberg parameters are shown in table I, and the coordinate frame can be seen in figure 11. It was necessary to control the end effector position to track the desired trajectory and the direction of the end effector to deposit material at a constant orientation. This can be formalised as a task variable $\sigma \in \mathbb{R}^n$, which is defined as:

$$\sigma(t) = \begin{bmatrix} x \\ y \\ z \\ \sigma_{fov} \end{bmatrix} = f(q(t)) \tag{6}$$

The variable $\sigma_{fov}$ is the error in the *field-of-view*, the vector pointing straight out of the end effector ($z_6$-axis in figure 11). The task variable differentiated with respect to time is given by:

$$\dot{\sigma}(t) = \frac{\delta f(q(t))}{\delta q}\dot{q}(t) = J(q(t))\dot{q}(t) \tag{7}$$

where $J(q(t)) = \frac{\delta f}{\delta q}$ is the Jacobian, and $\dot{q}(t)$ is the system velocity. The desired behavior of the robot is defined by $\sigma_{des}$. However, the robot is controlled in joint space, so an inverse kinematics approach is necessary to find the corresponding movement in joint space. It is proven that if the joint velocities track $\dot{q}_{des}$ as defined below, the task variable $\sigma$ will converge asymptotically to $\sigma_{des}$ [27]:

$$\dot{q}_{des} = J^\dagger \dot{\sigma}_{des} = J^\dagger(\dot{\sigma}_{des} + \Lambda\tilde{\sigma}) \tag{8}$$

where $\tilde{\sigma}$ is the task error, defined as:

$$\tilde{\sigma} = \sigma_{des} - \sigma \tag{9}$$

and $\Lambda$ is a positive definite matrix of gains. $J^\dagger$ is the right psudoinverse of $J$, which is the matrix satisfying the four Moore-Penrose conditions [28], $J^*$ being the complex conjugate of $J$:

$$JJ^\dagger J = J \tag{10}$$

$$J^\dagger JJ^\dagger = J^\dagger \tag{11}$$

$$(JJ^\dagger)^* = JJ^\dagger \tag{12}$$

$$(J^\dagger J)^* = J^\dagger J \tag{13}$$

The desired geometric trajectory that the end effector should follow, are given by the Cartesian coordinates that make up the first part of (6): $[x_{des}, y_{des}, z_{des}]^T$.

For the last element of (6), $\sigma_{fov,des}$, we control the *error* of the field-of-view, which is defined as:

$$\sigma_{fov} = \sqrt{(a_{des} - a)^T(a_{des} - a)} \tag{14}$$

where $a$ is the current orientation of the end effector, which corresponds to the vector $z_6$ in figure 11, and $a_{des}$ is the desired orientation. Because the field of view should be straight downwards, $a_{fov,des}$ is:

$$a_{fov,des} = \begin{bmatrix} 0 \\ 0 \\ -1 \end{bmatrix} \tag{15}$$

We wish for the error between the actual and the desired orientation to be zero:

$$\sigma_{fov,des} \equiv 0$$

$$\dot{\sigma}_{fov,des} \equiv 0$$

To express the desired end effector position in Cartesian coordinates, we rewrite the trajectory given in cylindrical coordinates (1)-(2) through the following transformation:

$$\begin{aligned} x_{des} &= r(\theta)\cos\theta \\ y_{des} &= r(\theta)\sin\theta \\ z_{des} &= z(\theta) \end{aligned} \tag{16}$$

Thus, the time derivatives are given as:

$$\begin{aligned}\dot{x}_{des} &= \dot{r}(\theta)\cos\theta - r(\theta)\sin\theta\dot{\theta}(\theta)\\ \dot{y}_{des} &= \dot{r}(\theta)\sin\theta + r(\theta)\cos\theta\dot{\theta}(\theta)\\ \dot{z}_{des} &= \dot{z}(\theta)\end{aligned} \tag{17}$$

where $\dot{r}$, $\dot{z}$, and $\dot{\theta}$ are defined in (3)-(5). Thus, the commanded joint velocity is defined in (8) with $\sigma_{des} = [x_{des}, y_{des}, z_{des}, 0]^T$ and $\dot{\sigma}_{des} = [\dot{x}_{des}, \dot{y}_{des}, \dot{z}_{des}, 0]^T$. We find the desired joint configuration $q_{des}$ by numerically integrating $\dot{q}_{des}$, and send this to the UR-5 dynamic controller via TCP-IP. This built-in controller ensures that the reference is tracked.

### C. Results

Material properties such as viscosity and density of the material used in this initial experiment put a height constraint on the structure to be built. In fact, the structure would collapse in on itself if it was built much taller than a critical height of a few centimetres. It was also necessary to adjust the vertical velocity of the nozzle. By reducing the height difference between layers, thereby making the nozzle press each layer down slightly while moving along the trajectory, the area of the contact surface between each layer was increased. This made the structure more stable, and less likely to collapse in on itself. This coincides with the approach chosen by Total Kustom, who also built layers that were three times wider than they were tall when printing the Concrete Castle [8]. Even with this modification, it was difficult to build steady structures that were taller than approximately 4 cm with the material that was used in our proof-of-concept experiment.

The beginning and end of the build was the most challenging part of the experiment. As mentioned, the extrusion of material was controlled by supplying compressed air to the caulking gun. Because the compressed air was controlled by a valve that had to be turned manually, turning the air on and off was a continuous process. The dynamics of this process greatly influence the flow of material. When turning the compressed air on, this meant that it was necessary to begin turning the valve approximately 10 seconds before the caulking gun would actually begin extruding material. In addition, the extrusion of material would change gradually, first extruding a small amount of material quite slowly, and then extruding more material quite quickly, depending on how much compressed air that was added. It seems reasonable that this extrusion process could be modelled by a time delay in series with a first or second order process.

When the build reached its end, it was also challenging to stop the extrusion of material. Naturally, the stopping process was also continuous, so it was necessary to time when to start closing the valve. If the valve was turned too early, so that the amount of material that was extruded was reduced while the robot was still following the build trajectory, the material would not adhere properly to the previous layer. Instead, it would be dragged after the manipulators end effector, pulling on the walls of the built structure, and this way increase the chances of the structure collapsing. When the valve was turned later, the caulking gun would still be depositing material when the end effector moved away from the build. Still, this was considered the best approach. The excess material was removed manually from the final structure straight after the build was done.

Fig. 12. **Test results:** The experimental work resulted in these small cups. It is evident that the width of the printed material, along with the height of the structure and the speed of the material deposition, are all important elements for the final result.

In summary, there are a number of parameters that was found to greatly influence the end result. Material properties such as density, viscosity and adhesiveness are important, but also the properties of the reference trajectory and the dynamics of the actuator, in this case the pressure controlled caulking gun, play a major role.

## V. CONCLUDING REMARKS

The initial proof-of-concept experiment along with the state-of-the-art review presented in this paper has shown that large-scale AM by robot manipulator is indeed possible, and has helped show some of the problem areas that need to be addressed in future work. Increasing the contact surface between each layer proved to be very helpful in order to increase the stability of the structure, and this will be necessary to include in later experiments. In the initial experiment, we achieved a larger contact surface by decreasing the height of each layer to make the nozzle press each layer down. A larger contact surface can also be achieved by changing the geometry of the nozzle, for example making it flat and elliptic, or even rectangular. Which approach to go for should be based on the material that is used, and on what kind of structure one is trying to build.

The starting and stopping point of the build will be challenging, especially when the extrusion of material is not controlled by a simple on/off-mechanism. It should therefore be a goal to create a better control mechanism for the flow of material. Even if it is not possible to stop or start the material flow momentarily, it might be possible to adjust the movement of the robot manipulator so that it works better with the material flow, for example making it slow down when it is close to the end.

In future work, a complete, full-scale system for AM by robot manipulator needs to have some way of monitoring the process, and to give feedback on whether or not the build is going as planned. What is expected to be a decisive aspect for robotised AM using CMT is the ability to compensate in real time for local welding defects such as local string collapse, and geometrical deviations from the building plan. In order to create an efficient system it will be necessary to design the control algorithms so that the system is able to compensate and correct weaknesses due to inaccuracies earlier in the build process. This initial experiment had a translation-only based trajectory, but in future experiment there should be more focus on the fact that the orientation of the robot's end effector can be controlled. The UR5 robot has 6 DOFs, which means that the manipulator can reach every point in its workspace with arbitrary orientation.

## ACKNOWLEDGMENTS

The work reported in this paper was based on activities within centre for research based innovation SFI Manufacturing in Norway, and is partially funded by the Research Council of Norway under contract number 237900.

## REFERENCES

[1] I. Gibson, D. W. Rosen, B. Stucker, *et al.*, *Additive manufacturing technologies*. Springer, 2010, vol. 238.

[2] rooiejoris.nl/"3D Elephant Petition", "3d elephant petition," 2015, accessed 2017-03-23. [Online]. Available: http://www.rooiejoris.nl/3d-elephant-petition/

[3] totalkustom.com/"News", "Total kustom news," 2014-2017, accessed 2017-03-26. [Online]. Available: http://www.totalkustom.com/news.html

[4] mx3d.xom/"Dragon Benches", "Mx3d - dragon benches," 2015, accessed: 2017-03-22. [Online]. Available: http://mx3d.com/projects-2/

[5] rooiejoris.nl/"Z Unlimited", "Z-unlimited," 2015, accessed 2017-03-23. [Online]. Available: http://www.rooiejoris.nl/z-unlimited/

[6] E. Malone and H. Lipson, "Fab@ home: the personal desktop fabricator kit," *Rapid Prototyping Journal*, vol. 13, no. 4, pp. 245–255, 2007.

[7] J. I. Lipton, D. Cohen, M. Heinz, M. Lobovsky, W. Parad, G. Bernstien, T. Li, J. Quartiere, K. Washington, A. Umaru, *et al.*, "Fab@ home model 2: Towards ubiquitous personal fabrication devices," in *Solid Freeform Fabrciation Symposium*, 2009.

[8] totalkustom.com/"3D Castle Completed", "Total kustom 3d castle completed," 2014-2017, accessed 2017-04-03. [Online]. Available: http://www.totalkustom.com/3d-castle-completed.html

[9] 3dprint.com/"3D-printed hotel suite", "3d-printed hotel suite," 2015, accessed 2017-03-27. [Online]. Available: https://3dprint.com/94558/3d-printed-hotel-lewis-grand/

[10] totalkustom.com/"Business Opportunities", "Total kustom business opportunities," 2014-2017, accessed 2017-03-26. [Online]. Available: http://www.totalkustom.com/business-opportunities.html

[11] 3dprint.com/"3D Concrete House Printer", "3d printer pre-order," 2017, accessed 2017-04-03. [Online]. Available: http://www.totalkustom.com/pre-order.html

[12] totalkustom.com/"Rudenko's 3D Printer", "Total kustom rudenko's 3d-printer," 2014-2017, accessed 2017-03-27. [Online]. Available: http://www.totalkustom.com/rudenko-s-3d-printer.html

[13] apis-cor.com/"ApisCor Bookbuyer", "Apis cor we print buildings," 2016, accessed 2017-04-02. [Online]. Available: http://apis-cor.com/files/ApisCor_BookBuyer_en.pdf

[14] apis-cor.com/"The first on-site house has been printed in Russia", "The first on-site house has been printed in russia," 2017, accessed 2017-04-02. [Online]. Available: http://apis-cor.com/en/about/news/first-house

[15] E. Barnett and C. Gosselin, "Large-scale 3d printing with a cable-suspended robot," *Additive Manufacturing*, vol. 7, pp. 27–44, 2015.

[16] P. Bosscher, R. L. Williams, L. S. Bryson, and D. Castro-Lacouture, "Cable-suspended robotic contour crafting system," *Automation in Construction*, vol. 17, no. 1, pp. 45–55, 2007.

[17] norsktitanium.com/"Norsk Titanium Technology", "Norsk titanium technology," 2015, accessed 2017-03-29. [Online]. Available: http://www.norsktitanium.com/wp-content/uploads/2016/07/Norsk_Titanium_Technology.mp4?_=1

[18] 3dprintingindustry.com/"US to Open Large-Scale Metal 3D-Printing Facility with Norsk Titanium", "Us to open large-scale metal 3d-printing facility with norsk titanium," 2015, accessed 2017-03-29. [Online]. Available: https://3dprintingindustry.com/news/us-to-open-large-scale-metal-3d-printing-facility-with-norsk-titanium-54236/

[19] Marcus Fairs, "Joris laarman works with opel," 2006, accessed: 23-06-2017. [Online]. Available: https://www.dezeen.com/2006/12/27/joris-laarman-works-with-open/

[20] jorislaarman.com/"Arm Chair", "Arm chair," 2015, accessed: 23-06-2017. [Online]. Available: http://www.jorislaarman.com/work/arm-chair/

[21] mataerial.com/"Gravity-Neutral 3D Printing", "Mataerial," 2013-2016, accessed 2016-12-13. [Online]. Available: http://www.mataerial.com/

[22] mx3d.com/"Bridge", "Mx3d bridge," 2015, accessed 2017-03-27. [Online]. Available: http://mx3d.com/projects/bridge/

[23] jorislaarman.com/"Butterfly Screen", "Butterfly screen," 2016, accessed 2017-03-27. [Online]. Available: http://www.jorislaarman.com/work/butterfly-screen/

[24] H. Zhang, J. Feng, P. He, B. Zhang, J. Chen, and L. Wang, "The arc characteristics and metal transfer behaviour of cold metal transfer and its use in joining aluminium to zinc-coated steel," *Materials Science and Engineering: A*, vol. 499, no. 1, pp. 111–113, 2009.

[25] S. Moe, G. Antonelli, A. R. Teel, K. Y. Pettersen, and J. Schrimpf, "Set-based tasks within the singularity-robust multiple task-priority inverse kinematics framework: General formulation, stability analysis, and experimental results," *Frontiers in Robotics and AI*, vol. 3, p. 16, 2016.

[26] Universal Robots, "Actual centre of mass for robot," 2016, accessed 2017-04-06. [Online]. Available: https://www.universal-robots.com/how-tos-and-faqs/faq/ur-faq/actual-center-of-mass-for-robot-17264/

[27] G. Antonelli, G. Indiveri, and S. Chiaverini, "Prioritized closed-loop inverse kinematic algorithms for redundant robotic systems with velocity saturations," in *Intelligent Robots and Systems, 2009. IROS 2009. IEEE/RSJ International Conference on*. IEEE, 2009, pp. 5892–5897.

[28] G. H. Golub and C. F. Van Loan, *Matrix computations*. JHU Press, 2012, vol. 3.